MAUSAM, **58**, 4 (October 2007), 481-500

551.515.2 : 551.508.826 (267)

Asymmetric structure of a severe cyclonic storm of North Indian Ocean as derived through INSAT OLR data

Y. E. A. RAJ, A. MUTHUCHAMI and RM. A. N. RAMANATHAN

Regional Meteorological Centre, Chennai, India

(*Received 29 January 2007, Modified 28 February 2007*)

e mail : yearaj@satyam.net.in

सार – इस षोध–पत्र में उत्तरी हिंद महासागर के भीषण चक्रवातीय तूफानों के दौरान मेघ संरचना में नियमित रूप से विषमता की मौजूदगी का अध्ययन 1993 से 2004 की अवधि में उत्तरी हिंद महासागर के दो बेसिनों में आए भीषण चक्रवातीय तूफान वाले दिनों में उपग्रह के बर्हिगामी दीर्घ तरंग विकिरण के आँकड़ों के तात्कालिक छः घंटेवार प्रेक्षणों के आधार पर किया गया है। 1999 की अवधि तक बर्हिगामी दीर्घ अवधि विकिरण आँकड़ों का विभेदन 2.5º × 2.5º तथा उसके बाद की अवधि का विभेदन 1º × 1º का था। भीषण चक्रवातीय तूफान के केंद्र को देखते हुए बर्हिगामी दीर्घ तरंग विकिरण का माध्य स्थानिक वितरण दो द्रोणियों और विभिन्न मौसमों के लिए प्राप्त किए गए। बर्हिगामी दीर्घ तरंग विकिरण के माध्य वितरण का अन्य समूह भी भीषण चक्रवातीय तूफानों की गति की दिषा के साथ प्रत्येक प्रोफाइल में घूमने के बाद उत्पन्न होता है। जब भीषण चक्रवातीय तूफान तट की ओर बढ़ते हैं तो भिन्न माध्य प्रोफाइल और पूर्व एवं पष्चिम की ओर बढ़ने वाले भीषण चक्रवातीय तूफानों का भी पता लग जाता है। अनेक मामलों में मेघ षीर्ष की ऊँचाई और विभिन्न दिषाओं में भीषण चक्रवातीय तूफानों के क्षैतिज विस्तार के आकलन किए गए हैं। इसमें विषमता के सूचकांक को परिभाषित किया गया है और विभिन्न वर्गों के लिए आँकड़े प्राप्त किए गए हैं।

अधिकांष वर्गों में माध्य बर्हिगामी दीर्घ तरंग विकिरण से भीषण चक्रवातीय तूफानों में नियमित विषमता का पता चला है। मानसून से पूर्व अरब सागर में आने वाले भीषण चक्रवातीय तूफान निम्न बर्हिगामी दीर्घ तरंग विकिरण का क्षेत्र दक्षिण पष्चिमी/पष्चिम अथवा बांई ओर के सुदूर क्षेत्र हैं। मानसून ऋतु के बाद पष्चिम/उत्तरी पष्चिमी क्षेत्र में भीषण चक्रवातीय तूफान के सबसे कम बर्हिगामी दीर्घ तरंग विकिरण के संकेत मिले हैं। यह पता चला है कि प्रायः तट से टकराने से पहले भीषण चक्रवातीय तूफान की तीव्रता थोड़ी कम हो जाती है। भीषण चक्रवातीय तूफानों की गति की दिषा और सामान्य पर्यावरणीय प्रवाह के होने से इस विषमता को समझा जा सकता है। कुछ विषेष मामलों में β - प्रभाव साधारण भूमिका निभाता है। बंगाल की खाड़ी में आने वाले चक्रवातीय तूफान विचाराधीन मौसम में अधिक तीव्र पाए गए है। इस श्रेणी में मानसून से पूर्व भीषण चक्रवातीय तूफान अधिक तीव्र पाए गए हैं।

ABSTRACT. The existence of systematic asymmetry in the cloud structure within the regime of Severe Cyclonic Storms (SCS) of North Indian Ocean has been studied based on instantaneous six hourly observations of INSAT Outgoing Long wave Radiation (OLR) data of SCS days for the period 1993 to 2004 for the two basins of north Indian Ocean. The OLR data was of 2.5° × 2.5° resolution for the period upto 1999 and was of 1° × 1° resolution for the subsequent period. The mean spatial distribution of OLR with reference to the centre of SCS was derived for the two basins and various seasons. Another set of mean distributions of OLR was also generated after rotating the individual profiles with reference to the direction of motion of the SCS. Separate mean profiles when the SCS approached the coast and for east and westward moving SCS were also derived. The height of cloud top for the various cases and the horizontal extent of SCS in various directions were computed. An index of asymmetry was defined and derived for the various categories.

Systematic and organised asymmetry in the SCS regime was detected from the mean OLR distributions in respect of most of the categories. For the pre-monsoon Arabian Sea SCS the sector of lowest OLR was the southwest / west or left rear sector. For post-monsoon SCS, the west / northwest sector reported the lowest OLR values for both the basins. It was found that generally the SCS slightly weakened in intensity prior to landfall. The asymmetry could be satisfactorily explained by invoking normal environmental flow and direction of motion of the SCS. The β – effect played modest role

in some specific cases. The Bay of Bengal SCS were found to be more intense for a given season. For a given basin pre-monsoon SCS were the most intense.

Key words – Outgoing long wave radiation, OLR, Severe cyclonic storm, Asymmetry, INSAT, β-effect, Secondary circulation, Bay of Bengal, Arabian Sea, Maximum wind, Environmental flow, motion vector.

1. Introduction

Tropical cyclones are intense atmospheric vortices, which originate over the tropical ocean and grow into vast whirling and rotating bands of winds, clouds and thundershowers. They are fed by energy and moisture supplied by the tropical ocean. The India Meteorological Department (IMD) defines a tropical cyclone as a low pressure area with associated maximum winds of at least 34 knots speed and upgrades the same to severe cyclonic storm (SCS) and very severe cyclonic storm (VSCS) if the associated wind speeds are 48/64 knots or more respectively (IMD, 2003a). Compared to their counterparts in Pacific and Atlantic Oceans, cyclones of North Indian Oceans are smaller in size and have shorter life span due to the restricted nature of basins where they originate and traverse but nevertheless frequently become as powerful and destructive as their larger and distant cousins. The internal structure of the tropical cyclones that form over different ocean basins of the world shows remarkable similarity despite differences in size and life period.

The three dimensional structure of a tropical cyclone has been extensively studied and documented (Anthes, 1982 and Asnani, 1992). The surface pressure is lowest at the centre of the cyclone and increases outward. The wind speed reaches its maximum value at nearly 40-80 km from the centre beyond which it decreases. The central parts are warmer than the surroundings and the temperature anomaly could be more than 10° K at the upper troposphere. The tropical cyclone grows upto a height of 10-15 kms. Generally concentric isobars and gradient wind balance are assumed, to model a cyclone at the surface level. Intense cyclones frequently develop an eye, which is a cloud free region at the centre of the storm characterised by the presence of subsidence.

Cyclonic storms exhibit specific configuration in cloud structure, which can be detected in the satellite cloud imageries in both visible and infrared bands. The classification of tropical cyclones by Dvorak, widely used by meteorological services all over the world is based on cloud imageries only (Dvorak, 1984). In the IR band the cloud imageries get defined based on the temperature profile at the cloud top of the storm field. Satellite on board receives energy in the infrared region as dictated by the cloud top temperature in the form of Outgoing Long Wave Radiation (OLR).

Asymmetries in the field of tropical cyclones in respect of parameters such as rainfall, cloudiness, winds etc., have been frequently observed even if the pressure field is axisymmetric. Such asymmetric features are apparently generated due to a host of synoptical and dynamical features. The asymmetric structure of the storm within its inner and outer cores (Elsberry, 1985) is of considerable scientific and practical interest. Detection of systematic asymmetry in the profiles of important parameters such as inflow, wind, convergence, vorticity, cloudiness etc., and understanding the physical reasons behind the generation of such asymmetry, besides leading to improved understanding of the dynamics of the cyclonic storm would also help in forecasting the cyclone parameters with better accuracy.

In respect of Pacific typhoons and Atlantic hurricanes, the RAWIN data obtained through aircraft reconnaissance conducted in the storm field when the systems are out at sea considerably augmented the satellite imageries and provided a deeper insight into the internal structure of storms. In respect of cyclones over Indian seas such aircraft reconnaissance data have not been generated. Satellite imageries from polar orbiting satellites were available to Indian meteorologists since 1970's and these were considerably helpful in tracking the cyclones. However the advent of INSAT series of geo-stationary satellites and their imageries and the availability of derived outputs such as OLR provided a quantum jump to not only cyclone tracking but also in the understanding of horizontal and vertical structure of the tropical cyclones over Indian seas. OLR is taken as a proxy for convection and is derived from the cloud top temperature sensed by the satellite. When we compare OLR data generated by polar orbiting *vis-a-vis* geo-stationary satellites, the latter is considerably superior to the former. The consistency of INSAT OLR data based on a single radiometer and the methodology of extraction has been discussed in detail by Kelkar *et al*., (1993), Rao and Kelkar (1989). According to Anthes (1982), tropical cyclones with eye are well organised for which features such as centre, maximum wind, curving cloud bands etc., are clearly defined. The eye forms only if the storm is very intense and is of atleast SCS intensity.

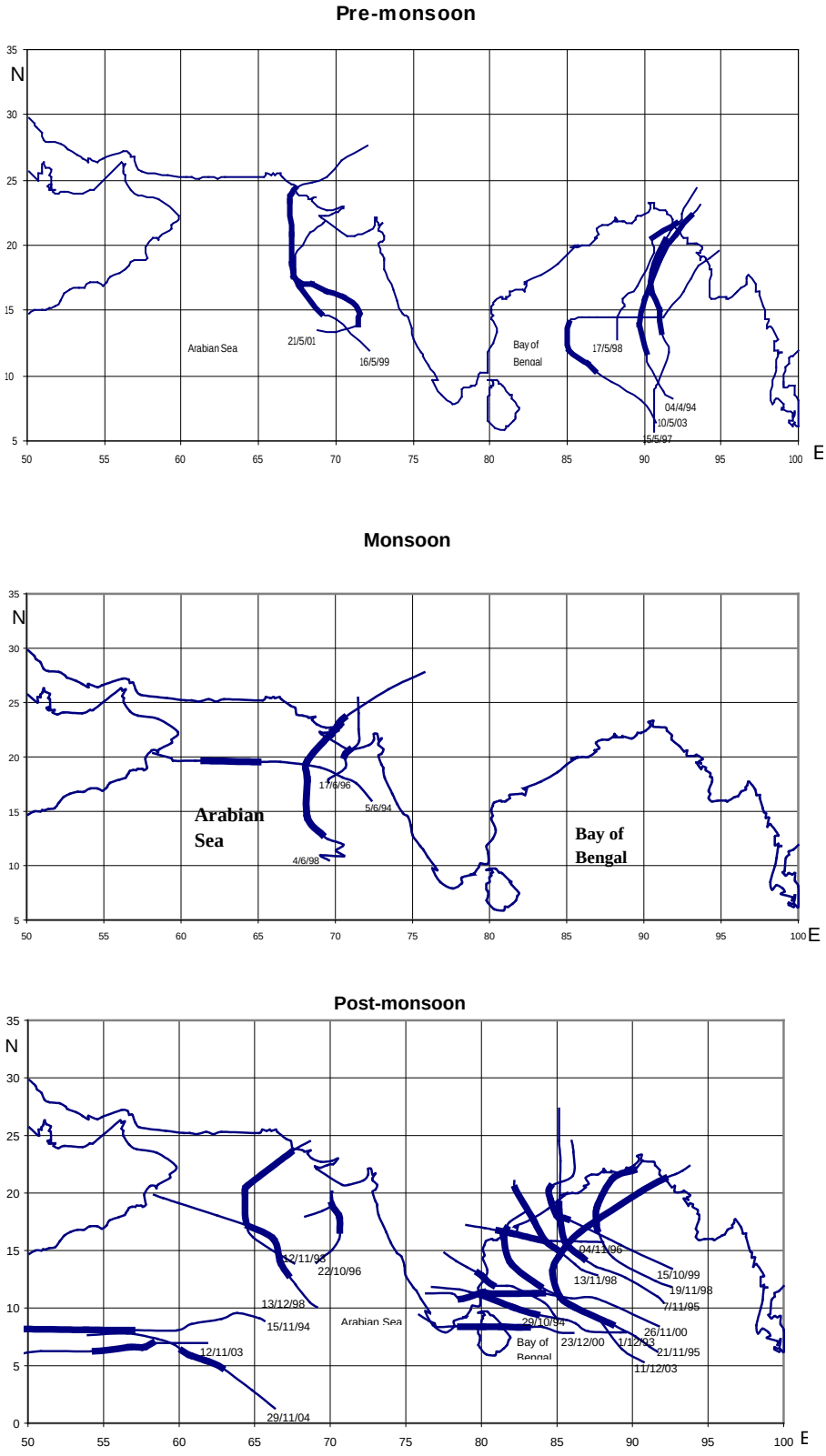

Fig. 1. Geographical location of India, Bay of Bengal and Arabian Sea and tracks of severe cyclonic storms (marked bold) considered in the study, displayed season wise

TABLE 1

Monthly frequencies of SCS over Indian seas during 1971-2005

	Month												
Basin	Jan	Feb	Mar	Apr	May	Jun	Jul	Aug	Sep	Oct	Nov	Dec	Total
BOB	1	0	0	4	13	1	0	2	5	11	30	8	75
AS	0	0	0	0	5	5	0	0	3	6	5	2	26

BOB – Bay of Bengal, AS – Arabian Sea, SCS – Severe cyclonic storm

TABLE 2(a)

Duration of low pressure systems and the number of SCS positions considered

S. No.	Duration of the system		Season	Basin of formation	No. of SCS positions considered at 0000 UTC, 0600 UTC, 1200 UTC, 1800 UTC
	From	To			
1	12 Nov 1993	15 Nov 1993	Post-monsoon	AS	1
2	01 Dec 1993	04 Dec 1993	Post-monsoon	BOB	3
3	29 Apr 1994	02 May 1994	Pre-monsoon	BOB	9
4	05 Jun 1994	09 Jun 1994	Monsoon	AS	1
5	29 Oct 1994	31 Oct 1994	Post-monsoon	BOB	3
6	15 Nov 1994	20 Nov 1994	Post-monsoon	AS	4
7	07 Nov 1995	10 Nov 1995	Post-monsoon	BOB	4
8	21 Nov 1995	25 Nov 1995	Post-monsoon	BOB	8
9	17 Jun 1996	20 Jun 1996	Monsoon	AS	1
10	22 Oct 1996	27 Oct 1996	Post-monsoon	AS	6
11	04 Nov 1996	07 Nov 1996	Post-monsoon	BOB	4
12	15 May 1997	19 May 1997	Pre-monsoon	BOB	9
13	17 May 1998	20 May 1998	Pre-monsoon	BOB	3
14	04 Jun 1998	10 Jun 1998	Monsoon	AS	12
15	13 Nov 1998	16 Nov 1998	Post-monsoon	BOB	1
16	19 Nov 1998	22 Nov 1998	Post-monsoon	BOB	3
17	13 Dec 1998	17 Dec 1998	Post-monsoon	AS	2
18	16 May 1999	22 May 1999	Pre-monsoon	AS	8
19	15 Oct 1999	19 Oct 1999	Post-monsoon	BOB	5
20	26 Nov 2000	30 Nov 2000	Post-monsoon	BOB	6
21	23 Dec 2000	28 Dec 2000	Post-monsoon	BOB	7
22	21 May 2001	28 May 2001	Pre-monsoon	AS	2
23	10 May 2003	19 May 2003	Pre-monsoon	BOB	9
24	12 Nov 2003	15 Nov 2003	Post-monsoon	AS	2
25	11 Dec 2003	16 Dec 2003	Post-monsoon	BOB	4
26	29 Nov 2004	02 Dec 2004	Post-monsoon	AS	1

TABLE 2(b)

Number of SCS and number of positions considered for different basins and seasons

Basin	Pre-monsoon		Monsoon		Post-monsoon		Total	
	A	B	A	B	A	B	A	B
BOB	4	30	0	0	10	48	14	78
AS	2	10	3	14	7	16	12	40
Total	6	40	3	14	17	64	26	118

SCS, BOB and AS – As in Table 1; A - Number of SCS; B - Number of positions

In this study the horizontal and vertical extent of cloud structure of SCS that formed over North Indian Ocean has been analysed based on INSAT OLR Data. The analysis has been conducted for the two basins *viz*. Bay of Bengal and Arabian Sea for the different seasons of India. The major objectives of the study are : to estimate the size and extent of an average SCS, to investigate asymmetry if any in the clouding in the inner region of the cyclone and if the asymmetry exists, to identify the physical causes behind the same. With the availability of nearly 12 years of INSAT OLR data as of now and the occurrence of adequate number of SCS over Indian Seas for different seasons for the same period, undertaking a study of this type has become possible.

2. Data and methodology

2.1. *Brief climatology of frequencies of SCS over North Indian Ocean*

Table 1 presents the monthly frequencies of SCS for Bay of Bengal and Arabian Sea for the 35-year period 1971-2005 (IMD, 1979 & 1996). A system was taken as an SCS even if it had maintained that intensity only for a brief period of time. As seen, the Bay of Bengal and Arabian Sea were respectively affected by 75 and 26 SCS yielding yearly frequencies of 2.14 and 0.74. The period January – March and July are by and large devoid of SCS. The months of November followed by May and October have the highest frequencies for Bay of Bengal. For Arabian Sea, October, November, May and June are the months with highest frequencies almost equally distributed across these months.

2.2. *SCS considered for the study and INSAT OLR data*

For this study we considered 26 SCS, which formed over Indian Seas and reached SCS intensity during the period 1993-2004. Tables 2(a) and 2(b) present the list of the 26 storms considered in chronological order and also the season wise break up. Fig. 1 presents the geographical location of India, the two basins of North Indian Ocean *viz*., Bay of Bengal and Arabian Sea and also the tracks of the 26 SCS. The portion of the track associated with the system maintaining intensity of SCS and above is identified by thick line. It must be noted that each storm considered, sustained the SCS intensity only for a limited period and during the reminder of its life cycle the intensity was lower such as cyclonic storm / depression.

The INSAT OLR data based on the IR imageries for the Indian region has been archived by the Satellite Data Centre, IMD. The instantaneous values of OLR have been generated at every three hours *viz*., 0000 UTC, 0300 UTC etc. as mean values averaged over 2.5° × 2.5° Longitude / Latitude grids for years upto 1999 and over 1° × 1° grids for the subsequent period. For the present study we have considered 4 OLR data sets for each day corresponding to 6 hourly observations at 0000 UTC, 0600 UTC, 1200 UTC and 1800 UTC. The total number of OLR observations at the above 4 hours of observation for the period of study with an SCS being present over the Indian seas was 118. The details of this break up are also provided in Tables 2(a) & 2(b). For the period when OLR data was available only in 2.5° square grid, the data was processed and the value at every 1° square grid was regenerated through spatial interpolation. Thus the derived data set provided OLR data at 1° grid either interpolated (1993 – 1999) or originally generated (2000 – 2004).

2.3. *Mean profile of OLR in the SCS field*

The mean profiles of OLR in the SCS field for different basins and seasons were generated through a number of steps as detailed below:

(*i*) The instantaneous OLR distribution around an SCS field for a given day and time was considered. The east-west (zonal) axis x and the south-north (meridional) axis y with degree longitude and latitude as the respective scales and (0, 0) corresponding to the centre of SCS, were defined. The OLR values in the area bounded by $-5<x<5$, $-5<y<5$ were interpolated at the grids (x,y) where x and y took the values –5, -4, …… , 0 ,……., 4, 5. Thus 121 values of grid point OLR data were generated around a given SCS centre. The map factor *viz*., the decreasing distance between longitudinal circles with increasing latitude has been ignored, the resulting error is below 5%.

(*ii*) The above computations were carried out only if the SCS centre lay over the ocean area. However in some cases some of the grid points within the SCS field might

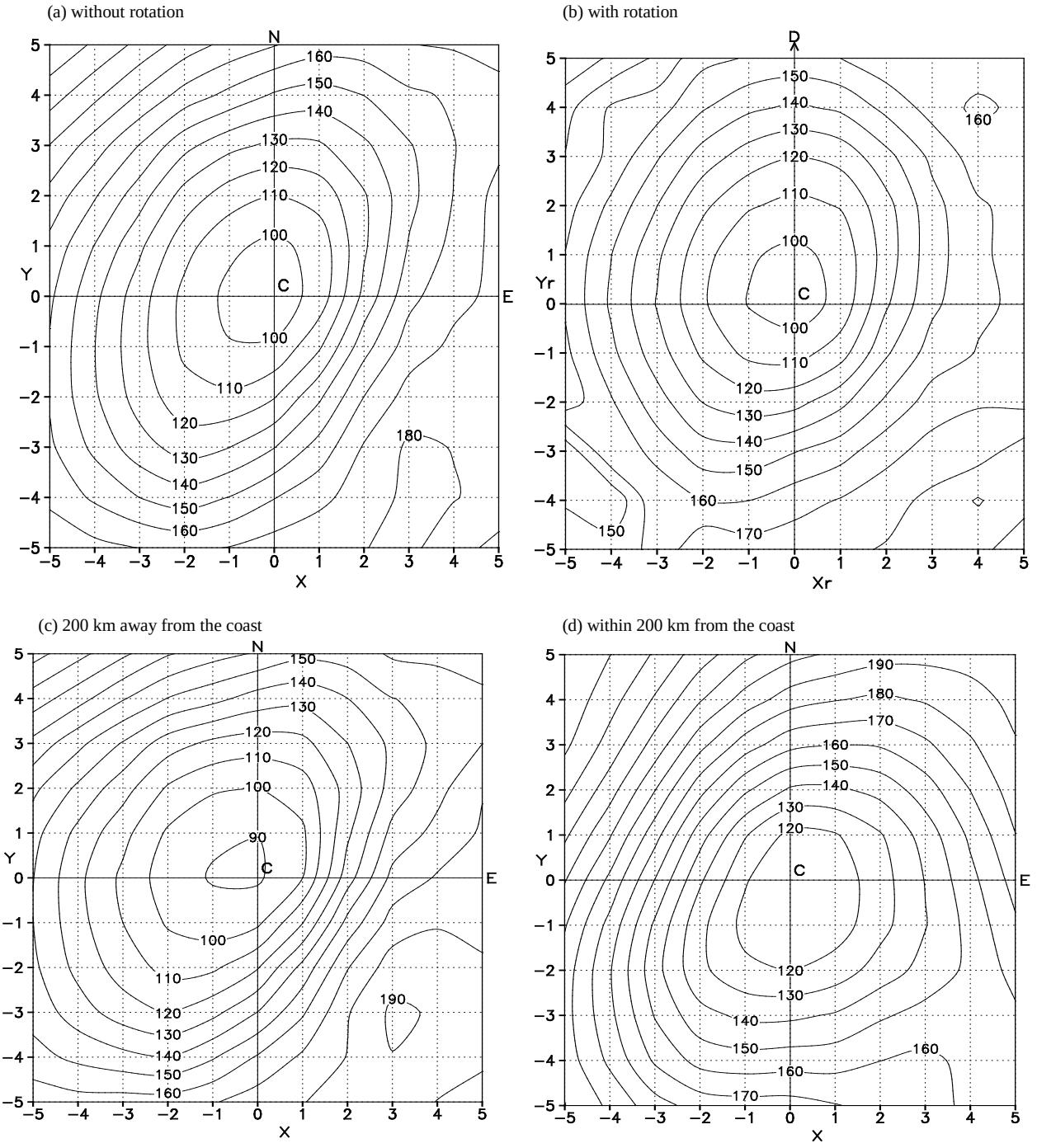

Figs. 2(a-d). OLR (W/m^2) distribution in SCS field, Bay of Bengal, Pre-monsoon season (March, April, May) X, Y, Xr, Yr axes; Scale - degree long / lat; C – Centre of the SCS (0,0); D – Direction of motion of the storm, aligned with Yr

have been located over the land area even if the centre was located over the ocean.

(*iii*) An average profile of OLR distribution around the centre of the SCS was then derived at the 121 grid points as defined above for each season and basin by averaging the various OLR spatial distributions.

(*iv*) Another type of OLR profile was computed by rotating the OLR values in the SCS field with reference to

TABLE 3

Details of lowest OLR and associated cloud top height in the SCS field for different seasons and basins

Season	Basin	Category	Number of SCS positions considered	Lowest OLR				
				Sector		Value (W/m^2)	Grid points lowest OLR	Associated cloud top height (km)
				WOR	WR			
Pre-monsoon	BOB	All	30	West	Front/Left Front	94	(0,0)	14.9
		>200 km	22	West/Northwest		88	(0,0)	15.4
		<200 km	8	South/Southeast		110	(0,0) & (0,-1)	13.6
	AS	All	10	West/Southwest	Left Rear	118	(0,0) & (-1,0)	13.1
		>200 km	5	Southwest/West		109	(-1,-1)	13.0
		<200 km	5	West/Southwest		117	(0,0)	13.1
Monsoon	AS	All	14	Southwest	Left Rear	108	(-1,-1)& (-2,-1)	13.1
Post-monsoon	BOB	All	48	West/Northwest	Front/Left Front	106	(0,0)	13.6
		>200 km	15	North/Northwest		100	(0,0)	14.0
		<200 km	33	West/Northwest		109	(0,0)	13.4
		Westerly	28	West/Northwest	Front	107	(0,0)	13.6
		Easterly	5	Northeast/North	Left/Left Front	107	(1,1)	13.6
	AS	All	16	North/Northwest	Front/ Left Front	125	(-1,1) & (0,1)	12.0
		>200 km	13	Northwest/West		123	(-1,1), (0,1) & (-1,0)	12.5
		<200 km	3	North/Northeast		133	(0,1)	11.7

BOB, AS, SCS – as in Table 1
WOR- without rotation, WR - with rotation,
> 200 km and < 200 km – SCS centre located greater than and less than 200 km from the coast respectively.

the direction of movement of SCS. This axis is defined as Yr and the axis perpendicular to Yr as Xr. Such rotation of axes was carried out for the OLR distribution of each SCS position and mean OLR profile for seasons and basins computed by averaging the rotated profiles.

(*v*) Mean profile of SCS with centres located 200 km away from the coast and 200 km within the coast were separately computed if sufficient number of cases were available.

(*vi*) For Bay of Bengal post monsoon SCS, separate OLR profiles were computed for SCS which moved westwards/eastwards.

(*vii*) The mean spatial distributions of OLR were derived for various basins and seasons with and without rotation for the various categories as defined above.

The purpose behind the above exercise of computing different types of OLR profiles is easily explained. The objective of the paper is to study the cloud profile around an SCS, and to detect any systematic asymmetry. The cloud distribution around a cyclone is known to be influenced by environmental mean flow, direction of cyclone movement, proximity of the cyclone to the coast etc. The effect if any of such mechanisms could be studied from the various mean OLR profiles.

3. Results and discussions

The mean OLR distributions thus derived for the various cases, basins and seasons are presented in Figs. 2-7. The results are also presented in Table 3 giving the sectors of lowest OLR, the lowest value of OLR and the grid points at which this lowest value has been realised. If the sectors are given as say west/northwest, it implies that OLR is lowest in the west sector, followed by the northwest sector. The sectors of lowest OLR are described as left/left front etc., with reference to direction of motion in respect of rotated profiles.

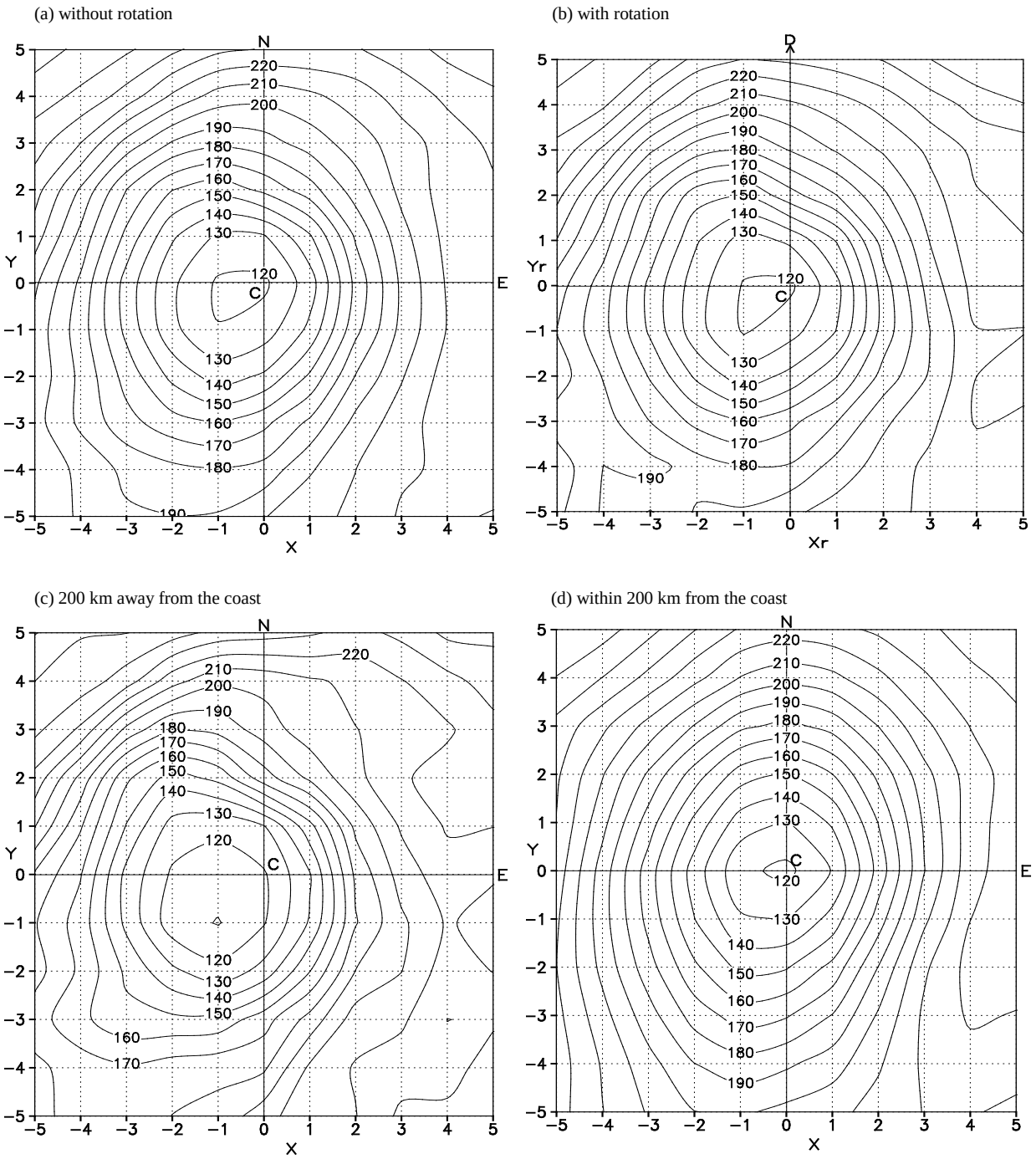

Figs. 3(a-d). OLR (W/m^2) distribution in SCS field, Arabian Sea, Pre-monsoon (March, April, May) (Foot notes as in Fig.2)

The representative nature of the sector of lowest OLR and the grid point at which the lowest OLR value has been reached as presented in Table 3 needs to be discussed briefly. Out of the 118 instances considered, only in 24 distributions or in nearly 20% cases, the lowest OLR was obtained at (0, 0) *i.e.*, at the SCS centre. In all the remaining 80% cases the lowest OLR was realised in the neighbouring grids only. This could have been due to real asymmetry in the cloud configuration and in some cases due to the inadequacy of the wide resolution of the OLR data as well. The sector of lowest OLR as given in Table 3 was also not realised in each and every case, but

(a) without rotation (b) with rotation

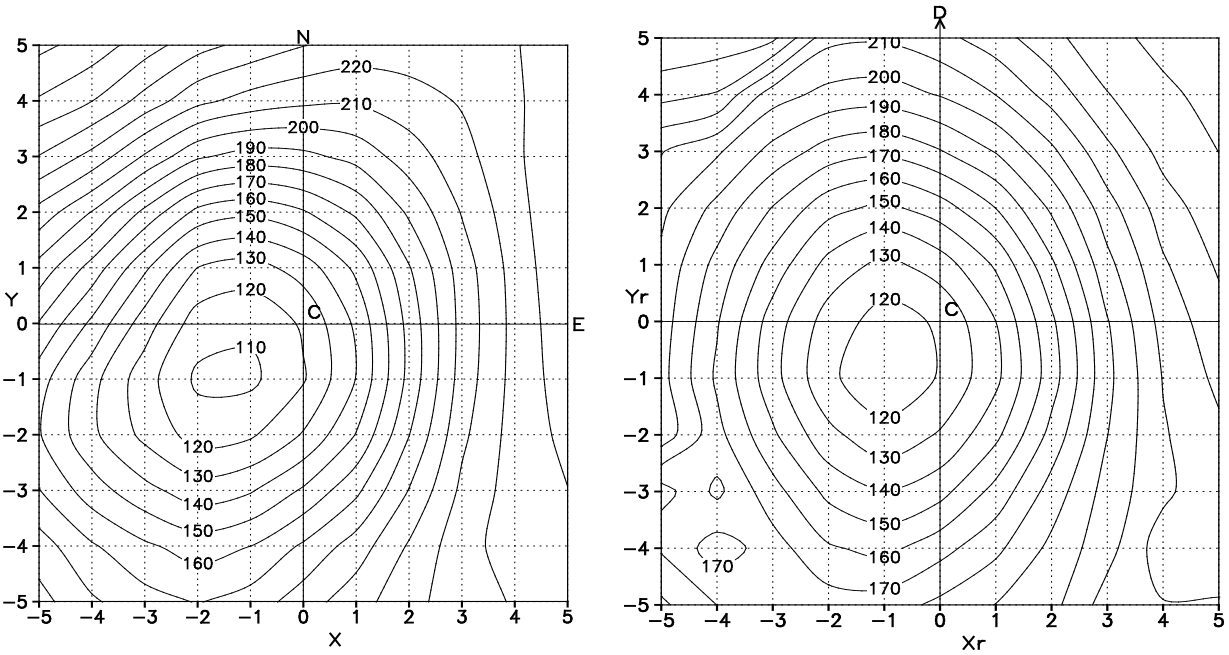

Figs. 4(a&b). OLR (W/m^2) distribution in SCS field, Arabian Sea, Monsoon (June, July, August, September) (Foot notes as in Fig. 2)

realised in a majority of cases. These aspects have to be taken into consideration while interpreting the results of Table 3. In what follows we discuss the salient features of mean OLR distributions season and basin wise.

3.1. *Pre-monsoon season*

3.1.1. *Bay of Bengal*

Figs. 2(a-d) present the mean OLR distributions in an SCS field over the Bay of Bengal for the pre-monsoon season during which 4 SCS (30 positions) formed and moved. From Fig. 2(a) which presents the non-rotated profile, it is seen that lower OLR values are obtained in the west/northwest sectors off the SCS centre. From Fig. 2(b), which presents the rotated profile, it is noticed that low OLR is found in the front/left front sectors of the SCS with reference to direction of motion. The mean OLR distribution (without rotation) when the SCS is at a distance of more than 200 km is depicted in Fig. 2(c). From this and Table 2 it is seen that the low OLR region is located west/northwest off the centre with 88 W/m^2 realised as the lowest OLR value. When the SCS approaches the coast low OLR region shifts to the south/southeast sectors. The lowest sector wise OLR increased to 94 W/m^2 when the SCS moved closer to the coast.

3.1.2. *Arabian Sea*

The OLR profiles based on data of 2 SCS (10 positions) are depicted in Figs. 3(a-d). The lowest OLR is obtained in the west/southwest sectors in all the distributions derived without rotation. With rotation the left rear sector has the lowest OLR.

3.2. *Monsoon season*

3.2.1. *Bay of Bengal*

Only one SCS formed, for which no data is available.

3.2.2. *Arabian Sea*

The OLR profiles are based on data of 3 SCS (14 positions) that formed and moved over Arabian Sea. Figs. 4(a&b) present the mean OLR distributions for non-rotated and rotated profiles. Fig. 4(a) reveals that the lowest OLR is realised predominantly in the southwest sector. From the rotated profile as presented in Fig. 4(b) the region of lowest OLR is the left rear sector with reference to the storm motion.

(a) without rotation

(b) with rotation

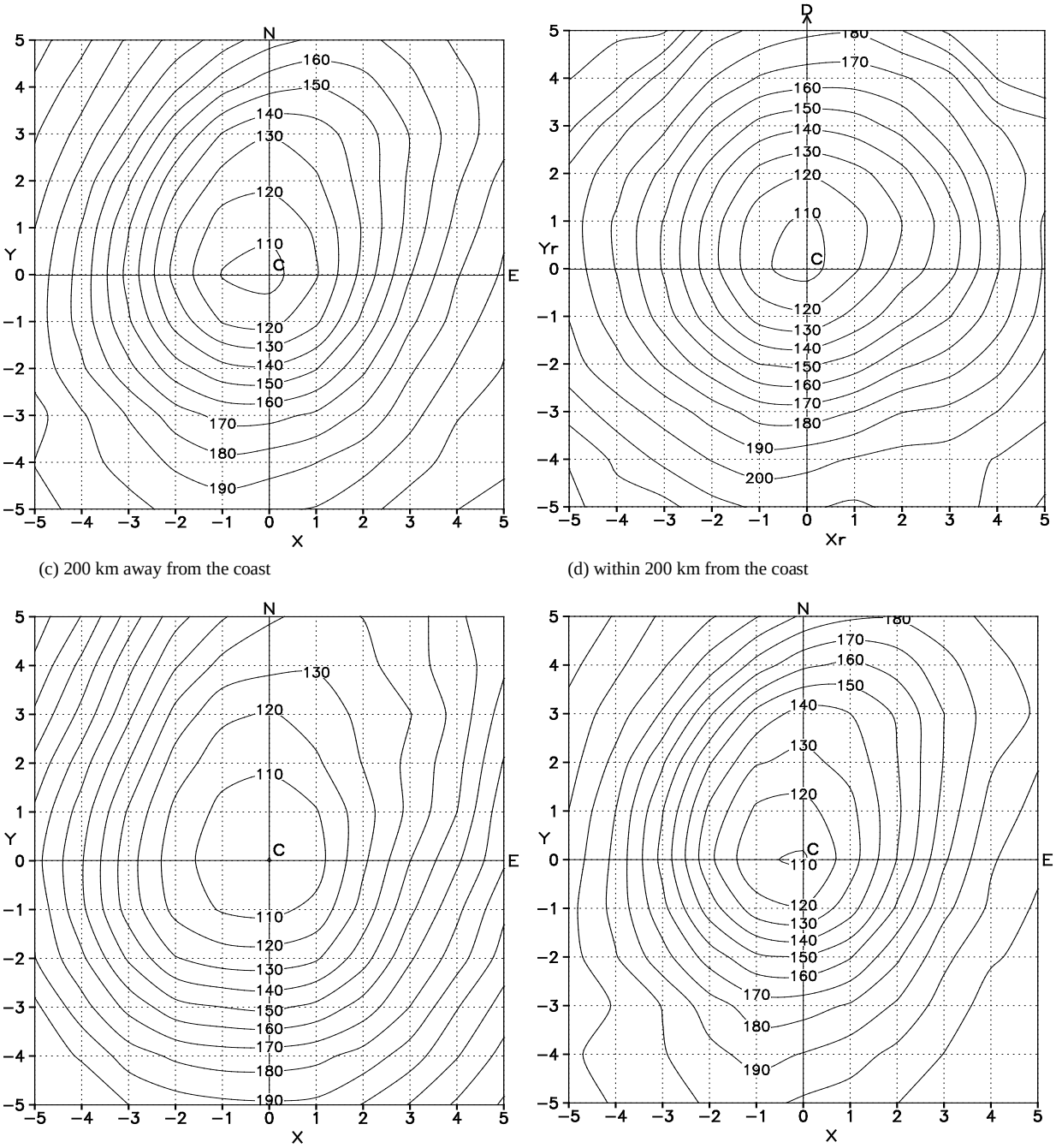

(c) 200 km away from the coast

(d) within 200 km from the coast

Figs. 5(a-d). OLR (W/m^2) distribution in SCS field, Bay of Bengal, Post-monsoon (October, November, December) (Foot notes as in Fig. 2)

3.3. *Post- monsoon season*

3.3.1. *Bay of Bengal*

The OLR profiles of SCS over Bay of Bengal during post-monsoon season based on 10 SCS (48 positions) for different categories are presented in Figs. 5(a-d). The lowest OLR is found in the west/northwest sectors with reference to the storm centre and in the front/left front sectors with reference to storm motion as revealed from Figs. 5 (a&b). Figs. 5 (c&d) present the OLR profiles when the SCS is 200 km away from the coast and within 200 km from the coast. From these figures and Table 3 it is seen that the lowest OLR value of 100 W/m^2 is realised

(a) without rotation, easterly movement

(b) with rotation, easterly movement

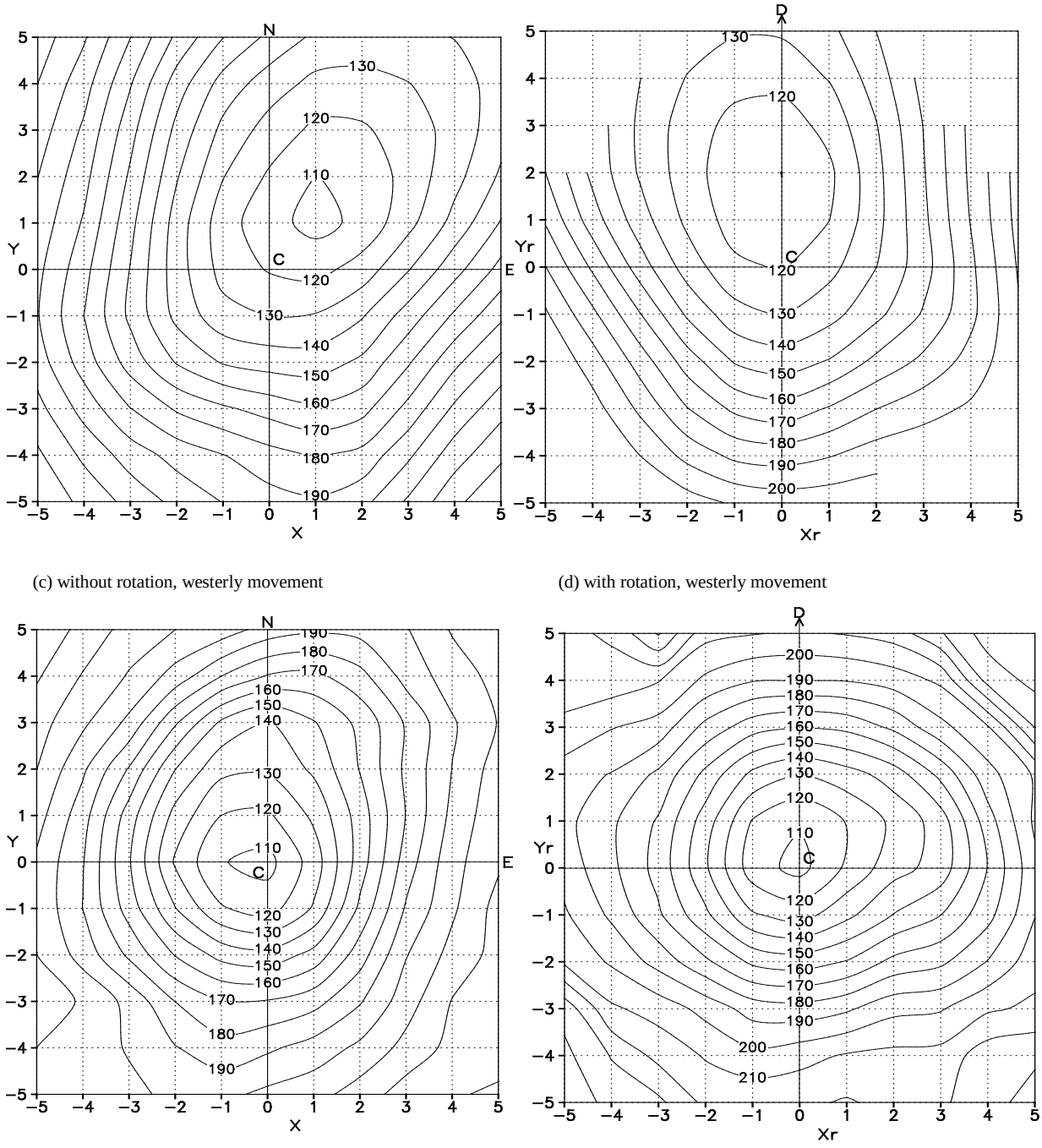

(c) without rotation, westerly movement

(d) with rotation, westerly movement

Figs. 6(a-d). OLR (W/m^2) distribution in SCS field, Bay of Bengal, Post-monsoon (October, November, December) (Foot notes as in Fig.2)

when the system is away from the coast only and when the SCS approaches the coast this increases to 109 W/m^2. In both cases the lowest sector wise OLR is realised in the northwest/west sectors of the storm.

Figs. 6(a&b) present the mean OLR profiles when SCS had easterly movement for non-rotated and rotated cases. When SCS moved towards west, lowest sector wise OLR is found in the northwest or front sector.

(a) without rotation

(b) with rotation

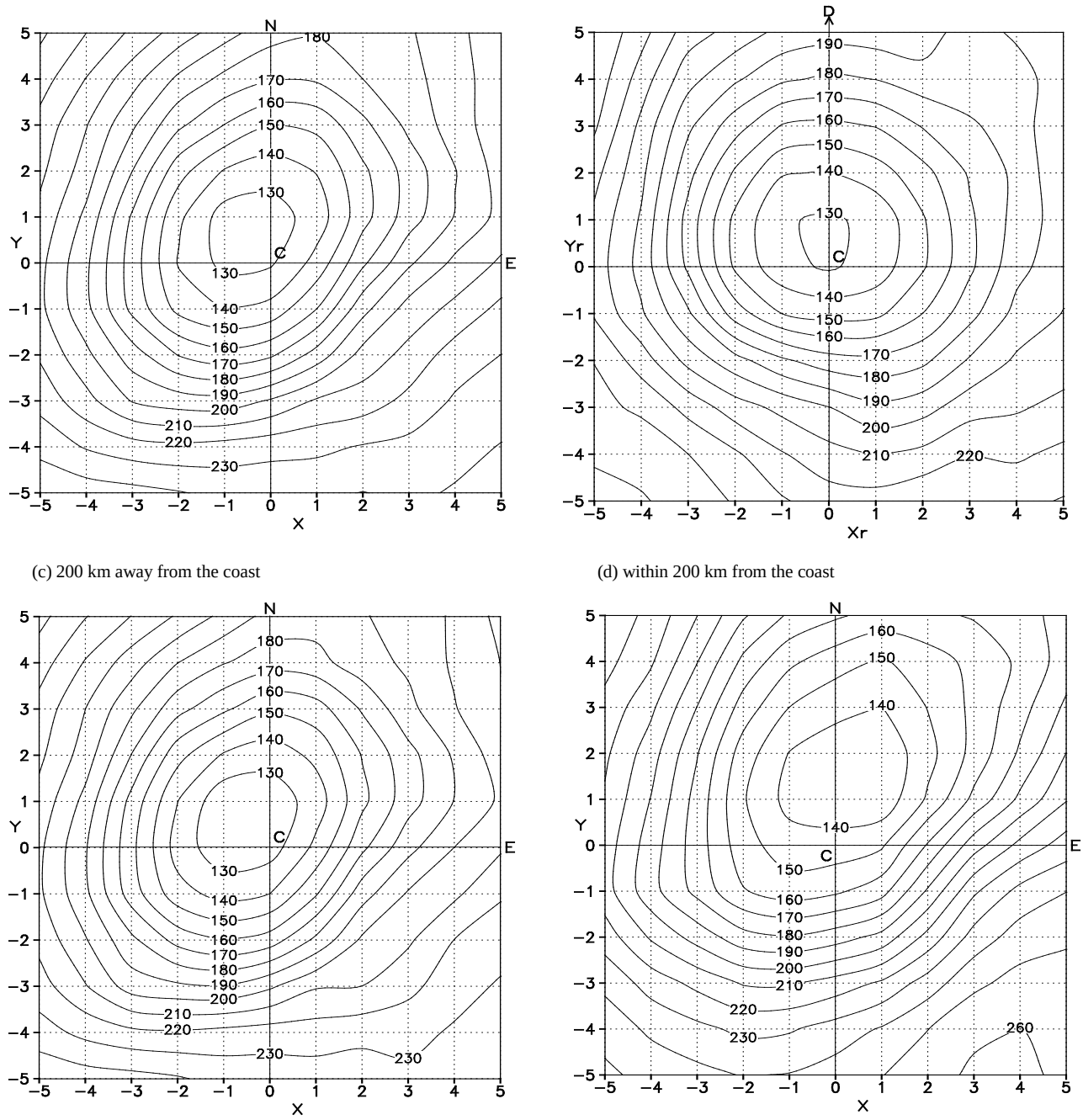

(c) 200 km away from the coast

(d) within 200 km from the coast

Figs. 7(a-d). OLR (W/m^2) distribution in SCS field, Arabian Sea, Post-monsoon (October, November, December) (Foot notes as in Fig.2)

Figs. 6(c&d) present the profiles for westerly movement, for which the lowest OLR values are found in the northeast or left front sector.

3.3.2. *Arabian Sea*

The OLR profiles of SCS over Arabian Sea during post-monsoon season based on data of 7 SCS (16 positions) for different categories are depicted in Figs. 7(a-d). The lowest sector wise OLR is obtained in the north/northwest sectors for the non-rotated profile and in the front/left front sectors for the rotated profile. The lowest OLR is 123 W/m^2 when the SCS is 200 km away from the coast and it increases to 133 W/m^2 when the system moves within 200 km off the coast. When the storm is 200 km away from the coast the lowest OLR is

TABLE 4

Mean latitudinal position of subtropical ridge at 200 hPa level in different months during post-monsoon season at 65° E and 90° E

Month	Mean latitudinal position at	
	65° E	90° E
October	17.0° N	19.5° N
November	11.5° N	14.5° N
December	8.0° N	11.0° N

found in the northwest/west sectors whereas it shifts to north/northeast sectors when the storm approaches the coast.

3.4. *Comparative study of OLR distributions corresponding to various seasons and basins*

3.4.1. *Distribution of lowest OLR and cloud top height*

Given the value of the OLR over a particular location, it is possible to estimate the temperature at the top of the cloud using Steffen–Boltzman law (Hess, 1959). Once temperature is estimated, the corresponding height, *viz*., height of the cloud top can be interpolated using the normal upper air sounding of the region considered. The cloud top height has been calculated for all the cases listed in Table 3 based on the normal soundings obtained from the NCEP/NCAR reanalysis website for the concerned ocean area. The mean height of the cloud top in the SCS field for different seasons and basins are also given in Table 3 from which we can draw several simple facts about the mean intensities of SCS for the different basins and seasons.

The Bay of Bengal SCS are more intense than the SCS of Arabian Sea for a given season. The pre-monsoon SCS are more intense than the SCS of other seasons for a given basin. The Bay of Bengal pre-monsoon SCS grow upto 15 km height and post monsoon SCS upto 14 km. The Arabian Sea SCS tower upto 13, 13, 12 km respectively during the pre-monsoon, monsoon and post-monsoon seasons. Slight decrease in the intensity is realised when the SCS approaches the coast.

Some physical reasons could be adduced to explain the above variation albeit to a limited extent. During pre-monsoon and post-monsoon seasons normal values of SST over the Bay of Bengal are 29.4° C and 27.7° C and over Arabian sea are 29.2° C and 27.6° C respectively. Each basin and the over lying atmosphere are warmer in pre-monsoon season compared to the post-monsoon season (IMD, 1988 & 2003b) which could explain the relative higher intensity of pre monsoon SCS. During monsoon season presence of strong easterlies at 10 km asl restricts the cloud growth beyond that height. Both during pre-monsoon and post-monsoon seasons the Bay of Bengal SCS grow taller than the Arabian Sea SCS by 10-15%. The normal SST values of these two basins do not differ substantially for a given season. It is however found that at 200 hPa the sub tropical ridge (STR) is located in a lower latitude over Arabian Sea than over Bay of Bengal by 2.5° - 3.0° latitude (Table 4; *source of data*: NCEP/NCAR website). Thus upper tropospheric westerly wind speeds are higher over Arabian Sea and such a feature is capable of restricting the vertical growth of SCS.

3.4.2. *Horizontal extent of cloudiness*

The OLR is taken as a proxy for convection and its value as an index of the vertical extent of clouding. The OLR values larger than 240 W/m^2 are associated with no clouding whereas the intervals 220-240, 200-220 and 180-200 W/m^2 are generally used to define different levels of increased cloud intensity. The OLR value of 200-220 W/m^2 is frequently taken to be associated with intense convection in tropics. However it appears justified to opt for a slightly lower value of OLR to delineate zones of intense convection in an SCS field for the following reason. Whereas normal tropical clouding associated with synoptic scale systems predominantly consists of cumulus cells and nimbus type of clouds, the clouding in an SCS field is characterised by vast sheets of organised high level cirrus out flow. Therefore, for the same intensity of clouding in the lower levels, vertical extent of clouding in an SCS regime is likely to spread to greater heights resulting in lower OLR. As such assigning a lower OLR threshold to delineate intense convection zone in an SCS regime appears reasonable and we have taken a value of 180 W/m^2.

As seen from Table 3, the mean lowest OLR value at the centre of an SCS falls well below 180 W/m^2. The radius of the region of SCS where the OLR values are below 180 W/m^2 abbreviated as ROLR180 and measured from the SCS centre has been derived for all cases (Figs. 2-7) along the directions north, east, south and west. The mean value is computed as the average of the four values. From these values, the extent of asymmetry in the SCS field can be conveniently defined based on an asymmetry index (AI), defined as

$$\text{AI} = \frac{\text{Maximum ROLR180} - \text{Minimum ROLR180}}{\text{Mean ROLR180}}$$

Table 5 presents the extent of cloudiness and the AI for the various cases. The pre-monsoon Bay of Bengal

TABLE 5

Mean ROLR180 (km) in an SCS field along various directions for different seasons and basins

Season	Basin	Category	Direction				Mean	AI (%)
			North	East	South	West		
Pre-monsoon	BOB	All	600	715	585	655	639	20
		>200 km	650	750	585	795	695	30
		<200 km	415	590	585	370	490	45
	AS	All	300	250	420	415	346	49
		>200 km	245	215	450	500	353	81
		<200 km	340	270	395	350	339	37
Monsoon	AS	All	305	245	510	555	404	77
Post-monsoon	BOB	All	585	390	410	420	451	43
		>200 km	925	505	475	535	610	74
		<200 km	515	340	360	375	398	44
	AS	All	520	285	260	390	364	71
		>200 km	490	290	270	400	363	61
		<200 km	600	260	200	360	355	113

ROLR180 – Radius of the region with OLR < 180 W/m^2
BOB, AS and SCS – as in Table 1, > 200 km and < 200 km – as in Table 3.
AI – Asymmetric Index

SCS is the largest with more than 600 km of ROLR180. This is followed by SCS of post-monsoon with a mean of 600 km when the SCS is over the high seas and 400 km when close to the coast. The Arabian Sea SCS are evidently smaller with ROLR180 ranging from 340-350 km only. The Bay of Bengal pre-monsoon SCS display modest asymmetry of 20% in the east-west direction with more clouding towards west.

For the Bay of Bengal post-monsoon SCS located over high seas ROLR180 extend as much as 925 km northwards from the centre of the SCS whereas the southward extension is only half of this (*i.e.*, 475 km). The large asymmetry of 74% reduces as the SCS approaches the coast but is still substantial with an AI value of 44%. When the SCS is close to landfall, the northward extension at 515 km is far greater than the southward extension of 360 km. This feature gets reflected in the rainfall pattern also when post-monsoon cyclones cross the east coast of India. The rainfall distributions in such cases extend substantially towards north than towards south. (IMD, 1973). The Arabian Sea SCS display large asymmetry in a relative sense, the AI values varying between 60-80% with ROLR180 more elongated towards south and west.

The size of a cyclone is defined in the literature (Willoughby, 1996) as the radius of the outer most isobar from the centre of the cyclonic storm or as the radius of isotach of 17 m/s or 34 kt which is the isotach corresponding to the minimum speed required for the system to be a cyclonic storm. According to Willoughby (1996) Pacific typhoons frequently exceed the size of 10° Long./Lat. An examination of satellite pictures of cyclonic storms presented in large number of IMD publications including Kalsi (2002) reveal that the extent of cloudiness in respect of cyclones of Indian seas frequently exceed 6° or 8° Long./Lat. even though the extension may not be uniform in all the directions.

4. Physical reasons that could be associated with the asymmetry in the field of SCS of North Indian Ocean

4.1. *Features associated with asymmetry in the field of an intense cyclone*

The surface pressure distribution in the field of a cyclonic storm is considered to be the most basic amongst the distributions of several other cyclone parameters. If

this is asymmetric, the skewed pattern could be expected to be reflected in the distribution of other related parameters such as, wind speed, vorticity, inflow and eventually clouding as well. Even if the pressure distribution were axisymmetric, the SCS may still manifest asymmetry in respect of the above mentioned parameters. By and large, the major mechanisms, which appear to be responsible for asymmetric cloud distribution in an SCS field are: (*i*) Environmental flow in the storm field, (*ii*) Movement of the storm, (*iii*) β – effect, (*iv*) Secondary circulations, (*v*) Modification of convection in the cyclone field when the system approaches the coast and (*vi*) A few other mechanisms such as variation in convection, SST, interaction with surrounding environment, boundary layer, etc. We briefly define and discuss some of the above mechanisms.

The superposition of the vortex into the environmental wind field in which it is embedded can cause substantial asymmetry in the cyclone regime (Holland, 1985). For example if a cyclone is embedded in a basic easterly current in the lower troposphere, the easterlies to the north of the cyclone centre would be stronger than the westerlies south of the centre. The environmental flow can modify the cyclone flow by increasing the wind speed in some sectors and by decreasing the speed in other sectors and also by changing the wind direction. Now in a cyclone with axisymmetric circular isobars, the isotachs also would be axisymmetric if gradient wind flow is assumed and frictional forces are not taken into consideration. The convergence would then be nil. When asymmetry is introduced due to environmental flow sectors of convergence and divergence develop. In sectors where the wind speed is relatively high curvature vorticity and evaporation from the ocean would be relatively large resulting in asymmetric distribution of these important parameters. The sectors of convergence and high wind speed normally are different and may not coincide.

The effect of movement of storm on the surface wind field of a cyclonic storm has been studied by Myers and Malkin (1961) and Basu and Ghosh (1987), using tangential and normal components of equation of motion in polar coordinates. Accordingly the motion vector of the storm influences the wind regime as given by the following equation:

$$\frac{v^2}{r} + fv = \frac{1}{\rho}\frac{\partial p}{\partial r} + \frac{vv_c}{r}\sin\theta \qquad (1)$$

where r is the radial distance from the centre of the storm, θ is the azimuthal angle measured clockwise from direction of motion, v and p are surface wind speed and pressure respectively at (r, θ), ρ is the density of surface air and f is the Coriolis parameter. If v_c is assumed 0 in Eqn. 1 we obtain the gradient wind equation. If v_g is taken as the gradient wind speed and f is assumed small we obtain the approximate equation

$$v = v_g + \frac{v_c}{2}\sin\theta \qquad (2)$$

Thus a wind speed profile with stronger winds in the right sector of storm (θ = 90º) than to the left sector (θ = 270º) in the cyclone field develops. The difference between these two extreme speeds is the speed of the storm. Such a pattern of wind speed could generate more convergence in the right forward sector of the storm besides generating more curvature vorticity and evaporation in the right sector.

The vorticity equation in a cyclone field for barotropic and non divergent flow is,

$$\frac{\partial \zeta}{\partial t} = -V.\nabla\zeta - \beta v \qquad (3)$$

Where ζ is the vertical component of relative vorticity, V is the horizontal wind vector, v is the meridional component of V, β = df/dy and f is the Coriolis parameter. The term βv contributes to the vorticity tendency with positive tendencies in the northern hemisphere west of the centre. This induces a tendency of the cyclone to propagate westwards. If non linear advection processes are introduced, cyclonic vorticity will be advected poleward. The net effect is movement of the cyclone in a northwesterly direction (Chan and Williams, 1987 & Holland, 1983) and generation of cyclonic gyre equatorward and west of the centre (Willoughby, 1996).

Secondary circulation is another important parameter responsible for creating asymmetry in a cyclone field. It is forced by an intense frictional destruction of angular momentum at the surface, weaker heating in the outer eye wall, extensive but weak cooling caused by frozen precipitation melting along the radar bright band, and similar extensive and weak heating due to condensation

TABLE 6

Effect of normal surface environmental wind flow and motion vector in the regime of a severe cyclonic storm

Month	Basin	dde	ffe	ddm	ffm	Sectors where Wind speed increased	Sectors of convergence
May	BOB	225	14	030	15	NE / E / **SE** / S / SW	S / **SW** / W
	AS	280	16	360	12	E / **SE** / S / SW / W	SW / **W** / NW / N
June	AS	250	31	315	12	NE / E / **SE** / S / SW	S / SW / **W** / NW
October	BOB N	150	08	315	15	N / **NE** / E / SE	E / **SE** / S / SW
	BOB S	230	11	315	15	NE / **E** / SE / S	S / **SW** / W
November	BOB	065	09	315	15	NW / **N** / NE / E	N / **NE** / E
December	BOB	065	16	315	15	W / NW / **N** / NE	N / **NE** / E / SE
October	AS	360	09	360	15	S / SW / **W** / NW / N	NW / **N** / NE
November	AS	035	11	360	15	W / NW / **N** / NE	NW / N / **NE** / E
December	AS	035	14				

BOB, AS – As in Table 1, N – North, S - South
dde, ffe – normal environmental wind at surface (speed in kmph)
ddm, ffm – normal speed of movement of SCS (speed in kmph)
Sectors are reckoned with reference to the centre of SCS
Underline implies wind speed / convergence reached maximum in that sector

and freezing in the anvil above the bright band (Willoughby *et al*., 1982, Marks and Houze, 1987). Muthuchami and Dhanavandhan (2005) concluded that if the heat source is in the inner side of the ring then advection of angular momentum will increase inside the ring and if it is in the outer side of the ring the advection of angular momentum will decrease inside the ring. Chan and Liang (2003) studied the change in the convective structure of a tropical cyclone during landfall and found that sensible heat flux has no appreciable effect while moisture supply is the dominant factor in modifying the convective structure.

4.2. *Asymmetry displayed by SCS of North Indian Ocean and possible causes*

4.2.1. In section 3 various types of systematic asymmetry in clouding present in the regime of SCS of North Indian Ocean as revealed from INSAT OLR distributions have been identified. We now look in to the possible physical causes behind the asymmetric profile based on known theories of asymmetry, some of which were discussed in the previous section. For the SCS of each category listed in Table 2(a), the most favourable zones of intense clouding corresponding to the various mechanisms discussed in Section 4.1 could be identified based on climatology of lower tropospheric wind pattern and movement of storm. As discussed, both environmental flow and motion vector of the storm modify the wind field of the storm. In Table 6 we present the normal wind flow in the surface level and normal motion vector of cyclones for the two basins for various months/seasons (IMD 1979, 1996 & 2003b). The environmental flow and the differential contribution of the motion vector of the storm, in various sectors as given in Eqn. (2) were super imposed into a hypothetical wind distribution in a cyclone field with concentric isotachs. The resultant wind vectors were computed for the various sectors. Table 6 presents the sectors where the wind speed increased after the superimposition and the resulting sectors of convergence. The sector where convergence reaches maximum is also indicated. In what follows, the asymmetry as obtained from the actual OLR data and the possible mechanisms are discussed season wise.

4.2.2. *Pre-monsoon season*

During the pre-monsoon season almost all the SCS belonged to the month of May only, for the period of

study (Table 1). The normal movement of Bay of Bengal SCS is near northerly and the lower tropospheric flow is southwesterly 14 kmph. The sectors with increasing wind speed or convergence do not exactly coincide with the west/northwest sectors where OLR maximum has occurred. The systems all have crossed the Bangladesh (Fig. 1) coast and this explains the shifting of sector wise cloud maxima to south/southeast sectors at the time of crossing.

For Arabian Sea SCS the OLR sector wise minima occurred in the southwest/west sectors when the systems are in the high seas and in the west/southwest sectors at the time of landfall. The normal surface winds over Arabian Sea in May are westerlies (16 kmph) and the normal movement of SCS considered is northerly. As seen from Table 6 the southwest sector generates increased wind speed and modest convergence due to the combined effect of environmental flow and motion vector. The beta effect generates more vorticity in the southwest sector. For systems over the high seas the lowest OLR at 109 W/m^2 is realised at the grid (-1,-1) and not at the centre (0, 0). This could have been partly due to a modest southwestward tilt in the SCS caused by the north-south temperature gradient which develops over Indian region prior to southwest monsoon. At the time of crossing the coast also the sector wise maximum of clouding is maintained but the OLR values in the northern sector decrease substantially by as much as 20-23 W/m^2 obviously due to generation of frictional convergence in that sector. For Arabian Sea SCS the rotated profile yields maximum sector wise cloudiness in the left rear sector. As the cases are fewer no firm conclusions could be reached on the effects if any on direction of movement and related clouding. For Bay of Bengal SCS no clear pattern of asymmetry emerged from the rotation.

4.2.3. *Monsoon*

During this season, SCS for which INSAT OLR data is available occurred in Arabian Sea only in the month of June. The movement and cloud structure of monsoon SCS are similar to the pre-monsoon SCS over Arabian Sea and the reasons for asymmetry are also by and large same *viz*., environmental flow, motion vector, beta effect and modest tilt southwards. The lowest OLR of 108 W/m^2 is realised at the grids (-2, -1) and (-1, -1) and not at (0, 0). With rotation the left rear sector has the maximum clouding, not just sector wise but as the lowest value in the regime as well.

The observed cloud pattern associated with Arabian Sea SCS of June has an obvious and remarkable similarity with the cloud pattern associated with the monsoon depressions that form over head Bay of Bengal and move westwards across the northern parts of India. The clouding in such cases is highest in the southwest sector of the depression with the centre of the clouding located substantially southwest of the depression centre. Some of the reasons attributed to the development of such a feature are: maximum pressure gradient south of the centre, tilt of the depression southwards, curvature correction to geostrophic flow etc. (Rao, 1976). The June SCS are more intense, basically warm core and move northwards, whereas the monsoon depressions are cold core and move westwards. Despite such differences in characteristics, there does appear to be some common mechanism such as tilt of the system which results in more clouding in the southwest sector in both the cases.

4.2.4. *Post-monsoon season*

For post-monsoon SCS the OLR sector wise minimum occurs in the north/northwest sectors for systems located in the high seas. For systems close to the coast the minimum occurs in the west/northwest sectors. The pre dominant wind direction is northeasterlies and the normal direction of movement is northwesterly. The northern sector registers the strongest wind speed besides generating convergence. The beta effect generates more vorticity in the southwest sector. When the system approaches the coast more frictional convergence is generated in the northwest sector than in the other sectors. Thus the sector wise preference for clouding is easily explained. With reference to the direction of motion, the front / left / left front sectors display the maximum sector wise clouding which is consistent with the profile obtained without rotation. For westerly moving systems the maximum clouding is obtained in the front sector and for northeast moving systems in the left / left front sectors. This shows that the cloud maxima also rotates when the systems recurve and that maximum convergence and inflow occurs ahead of the storm by and large confirming to findings by Shapiro (1983).

For post-monsoon Arabian Sea SCS also the north/northwest sectors display the maximum sector wise clouding. Environmental lower level wind flow and direction of motion apparently contribute to this asymmetry. When the systems are closer to the coast clouding increases in the northeastern sector due to frictional convergence.

4.2.5. The foregoing discussions bring out the plausible physical mechanisms behind the asymmetry observed in the cloud distributions in the regime of North Indian Ocean SCS. The asymmetry appears to have resulted from different mechanisms for different sets of SCS. For Bay of Bengal pre-monsoon SCS the asymmetry is not satisfactorily explained. In all the other cases the normal environmental flow and the cyclone motion vector have been able to explain the cause of the asymmetry to a reasonable extent. It also appears that environmental flow is the dominant factor compared to motion vector. The beta effect appears to exercise some influence in respect of the Arabian Sea systems. Though different physical mechanisms must have worked together generating asymmetric profiles of clouding in different sectors of the SCS, it is the integrated profile which is eventually observed. It is likely that particular mechanism may be predominant in respect of a particular category of SCS whereas it may play a minor role in respect of another category.

The representative nature of asymmetry detected needs to be discussed. The type of asymmetry and the sector of lowest OLR were derived for each and every one of the 118 cases studied and it was found that the pattern derived from the averaged data was reasonably representative though deviations were noticed as always expected. Again, if the effect of environmental flow and motion vector on the wind field of a given cyclone are to be investigated, the actual data of the above parameters for the exact date and time of the cyclone occurrence should have been taken into consideration. However the sectors associated with maximum inflow as given in Table 6 have been identified based on normal data only. Still the broader signal on the influence of environmental flow and motion vector on wind field should emerge. The deriving of a normal/average pattern also should filter out the 'noise', which would be invariably present in individual cases and bring out the signal, which is what is of interest.

The actual resolution of OLR data for the first part of the period of study is 2.5° × 2.5° and for the latter part is 1° × 1°. Though the former resolution is a bit wide for a study of this type, the broader signal on asymmetry should still emerge. The sectors of OLR minima as derived from both the data sets were compared and it was found that the asymmetric profiles as derived through the data of higher resolution compared very well with the profiles derived from data of lower resolution and also the average profiles presented in this study in the various figures and tables.

Finally the mechanisms adduced in this paper to explain the asymmetric profiles of cyclone of Indian seas are not advanced as an exhaustive lot. There could be a few other mechanisms also notably the influence of secondary circulations, the mechanisms of formation of convective rings, presence of mesoscale vortices, Rossby waves, boundary layer structure etc. Further if the surface pressure distribution itself is asymmetric, the skewness would be carried over to other parameters as well.

5. Summary

The results of the study are summarised below:

(*i*) By composting instantaneous INSAT OLR data for days during which an SCS was present over North Indian Ocean, systematic asymmetry in the mean cloud profiles in the regime of SCS field for different seasons and basins could be detected.

(*ii*) The SCS of Bay of Bengal during pre-monsoon season manifest the lowest sector wise OLR and hence intense clouding in the west/northwest sectors with reference to the centre and in the front/left front sectors with reference to the direction of motion.

(*iii*) The SCS of Arabian Sea during pre-monsoon and monsoon seasons manifest low OLR in the southwest/west and left rear sectors.

(*iv*) The SCS of Bay of Bengal during post-monsoon season are characterised by the presence of low OLR in the west/northwest and front/left front sectors.

(*v*) The SCS of Arabian Sea during post-monsoon season manifest lowest OLR in the northwest/west and front/left front sectors.

(*vi*) The mean radius of very intense convection and an asymmetric index based thereon have been computed for various season and basins. The AI varied from 20 to 77%. The SCS of Bay of Bengal have a horizontal extension of 640 and 450 km respectively during pre and post-monsoon seasons respectively. The SCS of Arabian Sea

spread upto 345, 405 and 365 km respectively during pre-monsoon, monsoon and post monsoon seasons.

(*vii*) The SCS of Bay of Bengal grow upto a mean height of 14.9 and 13.6 km respectively during pre and post-monsoon seasons. The SCS of Arabian Sea reach upto 13.1, 13.1 and 12 km respectively during pre-monsoon, monsoon and post-monsoon seasons. Thus Bay of Bengal SCS are more intense than Arabian Sea SCS given a season. For a given basin pre-monsoon SCS are more intense. Higher tropospheric temperature and SST are the possible causes for the higher intensity of pre-monsoon SCS, whereas strong upper tropospheric westerlies in the Arabian Sea appear to be the major cause behind lower intensity of Arabian Sea systems.

(*viii*) In all the categories the SCS decreased in intensity when they moved closer to the coast.

(*ix*) The normal environmental flow and the motion vector of SCS could explain the asymmetry in the cyclone regime in most of the cases. The β – effect appeared to play only a minor role in causing asymmetry. In the case of pre-monsoon and monsoon Arabian Sea SCS a discernable southwestward tilt with height also appeared to be one of the reasons for asymmetry.

Acknowledgements

The authors thank the Deputy Director General of Meteorology, Satellite Meteorology, India Meteorological department, New Delhi for having supplied the INSAT OLR data and the Deputy Director General of Meteorology, Regional Meteorological Centre, Chennai for having provided the facilities for the study.

References

Anthes, R. A., 1982, "Tropical Cyclones – evaluation, structure and effects", American Meteorological Society.

Asnani , G. C., 1992, "Tropical Meteorology", Noble Printers Pvt. Ltd., Pune.

Basu, D. K. and Ghosh, S. K., 1987, "A model of surface wind field in a tropical cyclone over Indian seas", *Mausam*, **30**, 183-192.

Chan, J. C. L. and Williams, R. T., 1987, "Analytical and numerical studies of the beta – effect in tropical cyclone motion, Part I : Zero mean flow", *J. Atmos. Sci.*, **44**, 1257-1264.

Chan, J. C. L. and Liang, X., 2003, "Convective asymmetries with tropical cyclone landfall. Part I : Plane Simulations", *J. Atmos. Sci.*, **60**, 1560-1576.

Dvorak, V. F., 1984, "Tropical cyclone intensity analysis using satellite data", NOAA, Technical Report.

Elsberry, R. L., 1985, "A global view of tropical cyclones", Proc. of International Workshop on Tropical Cyclone, Bangkok, Thailand, 1-12.

Hess, S. L., 1959, "Introduction to theoretical meteorology", 114-127.

Holland, G. J., 1983, "Tropical cyclone motion : Environmental interaction plus a beta effect", *J. Atmos. Sci.*, **40**, 328-342.

Holland, G. J., 1985, "A global view of tropical cyclones", Proc. of International Workshop on Tropical Cyclone, Bangkok, Thailand, 13-52.

India Meteorological Department, 1973, "Northeast Monsoon", FMU, Report No.IV – 18.4.

India Meteorological Department, 1979, "Tracks of storms and depressions in the Bay of Bengal and Arabian Sea".

India Meteorological Department, 1988, "Mean monthly averages (1971-1980) of Rawin Sonde/Rawin Wind data".

India Meteorological Department, 1996, "Tracks of storms and depressions in the Bay of Bengal and Arabian Sea - an addendum to Storm track atlas (1877 – 1970)".

India Meteorological Department, 2003a, "Cyclone manual".

India Meteorological Department, 2003b, "Marine climatological Atlas".

Kalsi, S. R., 2002, "Use of satellite imagery in tropical cyclone intensity analysis and forecasting – A guidebook for forecasters", Met. Monograph, Cyclone Warning Division, India Meteorological Department, Report No. 1/2002.

Kelkar, R. R., Rao, A. V. R. K. and Prasad, Sant, 1993, "Diurnal variation of outgoing long wave radiation derived from INSAT –IB data", *Mausam*, **44**, 1, 45-52.

Marks, F. D. and Houze, R. A., 1987, "Inner core structure of Hurricane Alicia from Doppler radar observations", *J. Atmos. Sci.*, **44**, 1296-1317.

Muthuchami, A. and Dhanvandhan, P., 2005, "The relation between size of the storm and the size of the eye", Predicting meteorological events, Mathematical approach, Narosa publishers, 102-113.

Myers, V. A. and Malkin, W., 1961, "National Hurricane Centre research Project", Report No 49, US. Dept. Commerce.

Rao, Y. P., 1976, "Southwest monsoon", Met. Monograph, No.1/1976, 107-185.

Rao, A. V. R. K. and Kelkar, R. R., 1989, "Estimation of precipitation and outgoing long wave radiation from INSAT –IB radiance data", *Mausam*, **40**, 2, 123-130.

Shapiro, L. J., 1983, "The Asymmetric boundary layer flow under a translating hurricane", *J. Atmos. Sci*., **40**, 1984-1998.

Willoughby, H. E., Clos, J. A. and Shoreibah, M. G., 1982, "Concentric eye walls, secondary wind maxima and evaluation of hurricane vortex", *J. Atmos. Sci*., **39**, 395-411.

Willoughby, H. E., 1996, "Global perspectives on Tropical Cyclones", TCP-38, WMO/TD No.693, 21-62.